Available online at www.sciencedirect.com

ScienceDirect

Materials Today: Proceedings XX (2016) XXX–XXX

www.materialstoday.com/proceedings

PMME 2016

Rheological Behavior of Polystyrene (PS)/Co-Al Layered Double Hydroxide (LDH) Blend Solution obtained Through Solvent Blending Route: Influence of LDH Loading and Temperature*

Kelothu Suresh, R. Vinoth Kumar, Rijumoni Boro, Manish Kumar and G. Pugazhenthi*

Department of Chemical Engineering, Indian Institute of Technology Guwahati, Guwahati 781039, Assam, India

Abstract

This investigation deals with the preparation of organically modified Co-Al layered double hydroxide (LDH) and influence of its loading and temperature on the rheological behavior of polystyrene (PS)/Co-Al LDH blends prepared via solvent blending method (SBM). Firstly, Co-Al LDH was synthesized by co-precipitation technique. Thereafter, PS blends with various LDHs content (3, 5 and 7 wt.% with respect to pure PS) were synthesized by SBM. The structural properties of the modified Co-Al LDH were characterized by XRD and FTIR analysis. The d-spacing value of modified LDH was found to be 2.8 nm by XRD analysis. The existence of sulfate groups in the modified LDH was affirmed by FTIR analysis. Rheological studies were done for the prepared samples in the shear rate array of 0.1-100 s^{-1} at various temperatures (20, 30 and 40 ^{o}C). It was observed that the rheology of PS solution is influenced by increasing Co-Al LDH loading, shear rate and temperature. All PS/Co-Al LDH blends showed an increment in their shear viscosity than pure PS. Also, the rheological data were fitted with different models, namely, Power law, Casson, Cross, Sisko, Herschel-Bulkley and Carreau models, to explain the rheological behavior. The results clearly indicated that Herschel-Buckley model displays good fit at lower temperature (20 ^{o}C), whereas Cross model offers best fit at higher temperatures (30 and 40 ^{o}C) for both pure PS and PS solution with various concentration of Co-Al LDH.
© 2016 Elsevier Ltd. All rights reserved.
Selection and Peer-review under responsibility of International Conference on Processing of Materials, Minerals and Energy (July 29th – 30th) 2016, Ongole, Andhra Pradesh, India.

Keywords: Co-Al LDH; PS; XRD; Rheology; Viscosity; Bias factor

* This is an open-access article distributed under the terms of the Creative Commons Attribution-NonCommercial-ShareAlike License, which permits non-commercial use, distribution, and reproduction in any medium, provided the original author and source are credited.
* Corresponding author. Tel.: 91-361-2582264; fax: 91-361-2582291.
E-mail address: pugal@iitg.ernet.in

2214-7853 © 2016 Elsevier Ltd. All rights reserved.
Selection and Peer-review under responsibility of International Conference on Processing of Materials, Minerals and Energy (July 29th – 30th) 2016, Ongole, Andhra Pradesh, India.

1. Introduction

Polymer-clay nanocomposites are one of the most vital modern technologies because of the capability of producing their unique new polymer properties. Therefore, nanocomposites have attracted considerable interest by many scientists of both industry and academia. The properties improvements include mechanical and high temperature durability [1], optical clarity [2], barrier properties [3] and reduced flammability [4]. Layered double hydroxide (LDH) is anionic clay, which is well characterized and conventionally used for catalysts [5], catalyst precursors [6], adsorbents [7], ion-exchangers [8], matrices for biosensors [9] and electrode modifiers [10]. The ideal formula of LDHs is represented as $[M^{2+}_{1-x} M^{3+}_{x}(OH)_2]^{x+}(A^{n-})_{x/n}\ mH_2O$ where M^{2+} represents divalent cations (M = e.g., Cu^{2+}, Fe^{2+}, Mg^{2+}, Co^{2+}, Zn^{2+} or Ni^{2+}) and M^{3+} represents trivalent cations (M = e.g., Al^{3+}, Fe^{3+}, Mn^{3+}, Ga^{3+}, Cr^{3+} or In^{3+}) . A^{n-} is an anion. The inorganic or organic anions (Cl^-, NO_3^- , ClO_4^-, CO_3^{2-}, SO_4^{2-}) are intercalated between the layers to hold the charge balance [11]. Until now, four techniques have been primarily utilized to prepare the LDHs, i.e., ion exchange, co-precipitation, hydrothermal and calcinations-rehydration (reconstruction) method [12]. Among these, co-precipitation method is extensively used to prepare LDHs. In this method, it can be prepared by mixing of alkali soda in salt solution. The resulting solution is aged at a required temperature [13]. LDHs are hydrophilic because of the presence of hydroxyl groups. LDHs, on modifying with appropriate organic molecules, become suitable for synthesizing polymer nanocomposites with non polar polymers [13].

Recently, many research groups have been working on polymer/LDH nanocomposites [1-4]. Different fabrication techniques were used for the polymer nanocomposite synthesis in order to study the structural, thermal and mechanical characteristics [1-4]. Qiu et al. [14] developed exfoliated PS/Zn-Al LDH nanocomposites via solution intercalation technique. They found that the thermal stability of exfoliated PS/Zn-Al LDH nanocomposites with 10 wt.% Zn-Al LDH to be 39 ^oC higher than that of pure PS at 50% mass loss was taken to be the point of reference. Qiu and Qu [15] prepared surfactant-free PS/LDH exfoliated nanocomposites using emulsion polymerization technique. Ding and Qu [16] also prepared the PS/Zn-Al LDH nanocomposites through emulsion polymerization with N-lauroyl-glutamate surfactants. Even at 10 wt.% Zn-Al LDH loading, they achieved completely exfoliated PS/LDH nanocomposites. He et al. [17] synthesized syndiotactic PS/Zn-Al LDH nanocomposites by SBM. It was found that nanocomposites with 1 and 3 wt.% LDH formed exfoliated and intercalated structures, respectively. The crystallization temperature of nanocomposites with 3 wt.% of LDH was 2 ^oC more than that of pure syndiotactic PS. Wang et al. [18] followed the in-situ bulk polymerization technique to fabricate PMMA nanocomposites with different quantity of LDH-U. According to the analytical method of Ozawa-Flynn, they reported that the degradation activation energies of these nanocomposites are higher as compared to pure PMMA. Du et al. [19] obtained nylon 6/Mg-Al LDH nanocomposites via melt intercalation of nylon 6 into part of organomodified Mg-Al LDH interlayers. Their XRD results demonstrated that too high LDH loading makes the LDH layers difficult to exfoliate. Zhang et al. [20] synthesized the ethylene-vinyl acetate copolymer (EVA)/Zn-Al LDH nanocomposties via melt and solution intercalation technique. The mechanical test demonstrated that the tensile strength (EVA/Zn-Al LDH) of the nanocomposites is 2.5-4.8 MPa higher than pure EVA.

The information of polymer solution is vital for the polymer processing industry. Understanding the solution rheology of polymers is important to develop suitable models for the solution polymerization procedure [21]. The rheological behavior of polymers is prime significance concerning of various polymer processing methods like extrusion, blow molding, injection molding, fiber spinning and calendaring. Polymer solutions have distinct industrial applications. Because of growing economic importance for manufacturing of polymers, it is essential to be considered the equipment and operational parameters for optimizing the design processes. The experiments using polymer blends are encouraging due to the addition of different polymers can offer various properties. However, it was observed that concentration and temperature mainly affect the rheological properties [22]. Besides the technological complexity of producing, handling and processing materials, a excellent broad information of their physical characteristics is required. Thus, the rheology is an essential quality control measure [23] and it is merely applied to study for liquid polymer solutions, blood, oil well drilling mud, paints and molten plastics. The rheological characteristics depend on flow index (n) and consistency index (K) utilized in the Power law model, in which K changes ubruptly with concentration of solution and applied temperature [24]. Several studies were reported that microscopic and mesoscopic clay fillers affected the rheological characteristics of the polymer blends [25, 26]. Ohta et al. [27] studied the rheological behavior of polyethylene (PE) for its utilization in the gel spinning

technology. They were investigated mainly on the shear flow viscosity of these solutions. They found that, such PE solutions exhibit a shear thinning behavior ranging a shear rate of 10^{-4} to 10^{3} sec^{-1}. Moreover, non-Newtonian behavior was more apparent with increasing the PE content in their solutions. Briscoe et al. [28] showed the influence of hydrogen bonding on the rheological behaviour of polyvinyl alcohol solutions (PVA). Their work revealed that the rheological behavior primarily depends on the relative strength of H_2 bonding present among the polymer chains along with water molecules. Perez et al. [29] studied the rheology of metallocene linear low density polyethylene (m-LLDPE) with linear density polyethylene (LDPE), and they used extrusion rheometry to analyze the effect of miscibility on practical rheology. Al-fariss et al. [30] studied the viscosity behavior of three types of Saudi Arabian crude oils as a function of shear rate at certain temperatures. The modified correlation proposed in this study has been found to fit the experimental data adequately for the crude oils as well as the polymer. They obtained the correlation via superposition approach. Kundu and Kundu [31] demonstrated that, the gelation depends on the wt.% ratio of methyl cellulose and surfactants which were present in the solution. Costa et al. [32] examined the linear viscoelastic characteristics of Mg-Al LDH nanocomposites with LDPE and HDPE and also approached the effect of LDH loading in the temperature range of 180-260 °C.

To our best knowledge, no research article allied to rheological behavior of PS/Co-Al LDH blends has been reported. Therefore the intention of the present study is to address the effect of LDH content and temperature on the rheological behavior of PS/Co-Al LDH blends solution derived by SBM. Different rheological models were studied to fit the obtained rheological data.

2. Rheological Models

Generally polymer based solutions are non-Newtonian in nature i.e. polymer mixture viscocity is not linearly related with shear rate. Usually, the nature of polymeric mixtures were shear thinning or the polymer solution and blends viscocity decrease by increasing shear rate. This can be explained by positioning a polymeric chain by applying a shear force. It is well known that at higher shear rate, the viscosity decreases due to the alignment of polymer molecules causing ease of flow of molecules. Different mathematical correlations are used to elaborate the shear stress versus shear rate of non Newtonian fluids. These correlations are facilitated to identify the flow characteristics and capability of a fluid to execute specific functions. Power law and Bingham plastic models are the two parameter models.

The power law model is expressed as:

$$\tau = K\,\gamma^{n} \quad (1a)$$

$$\eta = K.\,\gamma^{n-1} \quad (1b)$$

where, τ is shear stress, K is consistency index, γ is shear rate, η is apparent viscosity and n is flow behavior index or power law parameter. For a Newtonian fluid, n = 1; for shear thinning, n < 1 and shear thickening fluid, n > 1.

Bingham plastic model is stated as:

$$\tau = \tau_o + \gamma.\mu_p \quad (2)$$

μ_p is plastic viscosity, τ_o is yield stress.

There are numerous models that include three or more parameters. Third parameter helps to distinguish the fluid flow in the lower and upper Newtonian region as well as in the power law region. The plastic viscosity term is replaced in the Herschel-Bulkley model by adding power law expression.

Herschel-Bulkley model is stated as:

$$\tau = \tau_o + K\,\gamma^{n} \quad (3)$$

Sisko model [33] is used to articulate the flow behavior in upper Newtonian region and power law region. It is a three parameter model, which relates the apparent viscosity with shear rate.

$$\eta = \eta_\infty + K\gamma^{n-1} \quad (4)$$

Casson model [34] for non-Newtonian behavior is stated as:

$$\tau = \tau_o^{1/2} + \eta_\alpha\,\gamma^{1/2} \quad (5)$$

where, η_α is viscosity at infinite shear stress.

The models used to express polymer solutions, food, activated sludge and blood flow chateristics are Cross and Carreau models. Each model consists of four parameters.

Cross model is given as [35]:

$$\eta = \eta_\infty + [(\eta_o - \eta_\infty) / (1+ (C * \gamma)^m)] \quad (6)$$

where, m is dimensionless exponent and C is time constant. η_o and η_∞ denote the initial viscosity at zero shear rate and final viscosity at infinite shear rate, respectively.

Whereas Carreau model is stated as [36]:

$$\eta = \eta_\infty + [(\eta_o-\eta_\infty) * (1+ (\lambda * \gamma)^2)^{(n-1)/2}] \quad (7)$$

λ and n correspond to relaxation time and gauge of shear thinning properties, respectively.

The standard error (SE) equation is incorprated to fit the model with the obtained experimental results as described below [37]:

$$SE= (\sum(y_m - y_c)^2 / (n-1))^{1/2} \quad (8)$$

where, n is number of data point, y_c is predicted value and y_m is experimental value at every data point. The Bias factor (B_f) provide a further new information about the deviation of experimental with predicted values. B_f = 1 represents that experimental values are coincided with predicted values.

The Bias factor is expressed as [38]:

$$B_f = 10^{[\sum \log (y_c / y_m) / n)]} \quad (9)$$

Experimental *vs* predicted viscocity plot can be confirmed from a SE calculation and B_f.

3. Experimental

3.1. Raw material

Polystyrene was procured from National Chemicals, India. Cobalt nitrate ($Co(NO_3)_2.6H_2O$), aluminum nitrate ($Al(NO_3)_3.9H_2O$), sodium hydroxide (NaOH), sodium dodecyl sulfate (SDS) ($NaC_{12}H_{25}SO_4$), xylene (C_8H_{10}) were obtained from Merck (I) Ltd., India.

3.2. Synthesis of organomodified Co-Al LDH

Co-precipitation technique was used to synthesize Co-Al LDH. The salts, cobalt nitrate, aluminium nitrate and SDS were taken in the ratio of 2:1:1.5, respectively to form an aqueous solution using Millipore water obtained from Milli-Q system. After which, NaOH (2 M) was supplemented drop by drop followed by stirring of solution until it reach a pH level of 8.5. The consequential mixture was stirred continuously for 16 h at atmospheric conditions. The final precipitate was subjected to filtration and washing with Millipore water until attain a neutral filtrate. Further, it was allowed to keep at ambient temperature up to 12 h. The precipitate was transferred in to a Petridish and dried at 70 ^oC for 16 h using hot air oven (Make: Reico, Model: ROV/DG) to remove moisture. Dried LDH was pulverized into powder form for further use. Fig. 1 depicts the schematic of synthesis of Co-Al LDH.

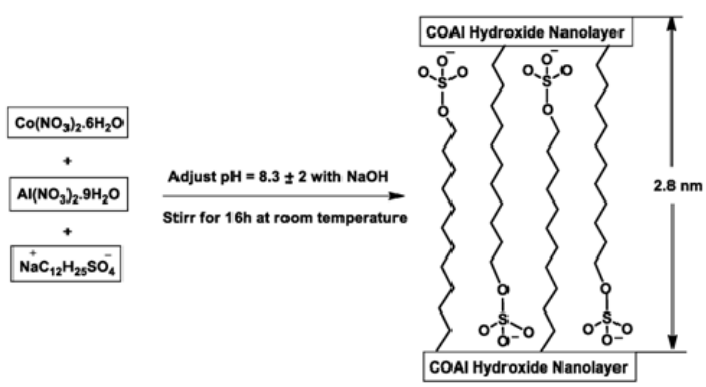

Fig. 1. Schematic representation for synthesis of Co-Al LDH

3.3. Synthesis of PS/Co-Al LDH blend solution

PS/Co-Al LDH blend was prepared in xylene (Table 1). Prior to synthesis, PS and organically modified Co-Al LDH were dried for 12 h at 60 and 70 ^{o}C, respectively in a hot air oven to remove the adsorbed moisture content. Firstly, a required amount of LDH was added in 109 mL of xylene and continuously allowed to stir for 24 h. Further, calculated quantity of PS was added in the prepared LDH solution and again allowed to stir for 12 h at atmospheric conditions. The pure PS solution was synthesized by following the similar process in the absence of Co-Al LDH. The resultant PS and PS/Co-Al LDH blend solution was taken immediately for rheological analysis. Note that, all the solutions are designated as pure PS, PS 3, PS 5 and PS 7 for polystyrene, PS/Co-Al LDH (3 wt.%), PS/Co-Al LDH (5 wt.%) and PS/Co-Al LDH 7 (wt.%), respectively.

Table 1. Preparation chart for PS/Co-Al LDH blend solution

Sample Name	LDH loading (wt%)	LDH (g)	Solvent (ml)	Solvent (g)	PS (g)
PS	0	0	109	95	5
PS 3	3	0.15	109	95	4.85
PS 5	5	0.25	109	95	4.75
PS 7	7	0.35	109	95	4.65

3.4. Characterization

X-ray diffraction (XRD) pattern of organomodified Co-Al LDH was measured at ambient condition by X-Ray Diffractometer (AXS D8 ADVANCE Powder, Bruker) equipped with Cu-Kα radiation (λ= 1.5406 Å). The patterns were recorded in the rage of 2-50° with scanning speed of 0.02°/s. The FTIR spectrum of LDH was obtained by Perkin Elmer Fourier transform infrared spectroscopy, which cast on potassium bromide (KBr). The measurements were taken in the wave region of 4000-400 cm^{-1} at the room temperature. Rheological measurements were conducted on a rotational rheometer, Physica MCR 301 (Anton Paar), by parallel plate geometry with 50 mm of radius. The parallel plate rheometer comprises two parallel with circular plates, in which one of them stationary, whereas the other one rotates. Rheological studies were carried out in the shear rate ranging between 0.1 s^{-1} and 100 s^{-1}. Fresh samples were used for each measurement at temperatures of 20, 30 and 40 ^{o}C.

4. Results and discussion

4.1. XRD analysis

XRD is a most powerful tool for characterizing the level of crystallinity of materials and sorts of layered structures, i.e. exfoliated and/ or intercalated, as the peak varies with the gallery height of the LDH. Fig. 2 shows the XRD graph of organomodified Co-Al LDH, where the d spacing of the Co-Al LDH is evaluated as 2.8 nm (2θ = 3.14^{o}) from Bragg's Law, $d = n\lambda/2\sin\theta$. This value signifies the brucite like layer's thickness (see Fig. 2). It is supposed that a larger space between Co-Al nanolayers that endorse the intercalation of the polymer molecules and also increase compatibility among organomodified Co-Al LDH and polymer molecules. It leads to easy exfoliation of the stacking Co-Al layers in the polymer matrix to form well dispersed polymer/LDH blends.

4.2. FTIR analysis

The surface functional groups of the LDH were further revealed by FTIR spectrum. Fig. 3 illustrates the FTIR spectrum of organomodified Co-Al LDH. The broad band attained at 3500 cm^{-1} is accredited to the O-H stretching of hydroxyl group of LDH [39]. A broader peak at wavenumber of 1630 cm^{-1} represents to the existence of δ (H-OH) [14]. An intense peak is observed at 1218 cm^{-1} which is assigned as symmetric vibration of sulfate from

dodecyl sulfate anion. The peak at wavenumber of 1063 cm^{-1} is designated as asymmetric vibration of sulphate from dodecyl sulfate. Three prominent peaks attained in the region of 2848, 2920 and 2957 cm^{-1} are designated as C-H stretching vibration [40]. Guo et al. [40] also achieved C-H stretching vibration at these particular wavenumbers. The bands seen at lower frequency region signify lattice vibration modes and it can be attributed to M-O and M-O-M from 800 to 450 cm^{-1} (where M = Co, Al) in the LDH sheets [41-42].

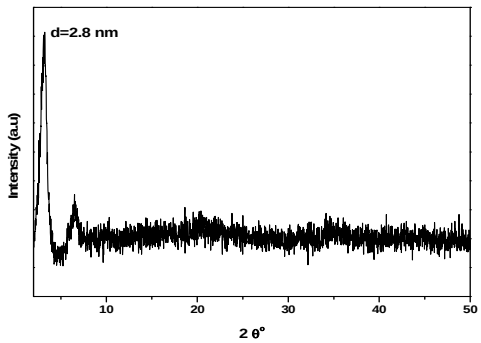

Fig. 2. XRD patterns of organomodified Co-Al LDH

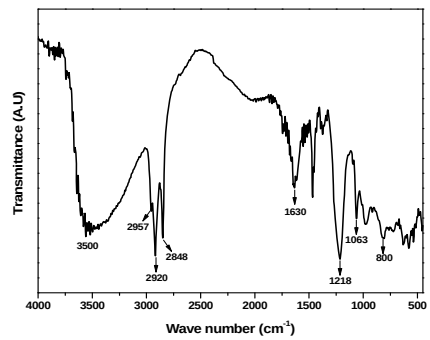

Fig. 3. FTIR spectrum of organomodified Co-Al LDH

5. Rheological study

5.1. Effect of Co-Al LDH

The polymer solution viscosity mainly relies on a various factors that include molecular weight, molecular shape and polymer molecules interaction with the solvents. Furthermore, the viscosity of solution depends on the dissolved polymer concentration. In this study, pure PS and PS solution with various concentration of Co-Al LDH was prepared to study its effect on loading with shear stress and viscosity by changing the shear rate. The influence of LDH content on shear stress versus shear rate for pure PS and PS/LDH solution is illustrated in Figs. 4-6. The trends in rheological analysis demonstrate that the investigated pure PS and PS/LDH solutions behaves in a non-Newtonian manner as revealed by the decrease of the solution viscosity when the shear rate increases (see Figs. 4-6).

Under the application of the shear stress, the alignment of the polymer molecules can take place and it allows easy to flow of the molecules, which declines the viscosity at higher shear rates. This is referred as “shear thinning fluid” (pseudo plastic). It is very clear from Figs. 4-6 that the viscosity decreased more rapidly at lesser shear rates than at higher shear rates. It is also observed that as the content of LDH increases, solution viscosity also increases due to the increased LDH particle interaction with PS matrix that makes it more difficult to flow.

5.2. Effect of temperature

The variation of viscosity and shear stress with shear rate was examined for the pure PS and PS/ Co-Al LDH blend solution at temperature of 20, 30 and 40 ^{o}C. As evidenced from Figs. 7-10, there is a decrement in dispersion shear stress because of increase in temperature. The shapes of the curves are as per the nature of the plot in the figures. The level of the curve reduces with an increase in the temperature. This proves that at every temperature, for a material, a separate generalized Ostwald curve must be followed. The viscosity rises with increasing Co-Al LDH content of the solution. Similarly, at higher loading (> 7 wt.% LDH), the polymer solution flow decreases regardless of its temperature. From the figures, surge in viscosity is observed with an increase in the Co-Al LDH concentration at all temperatures.

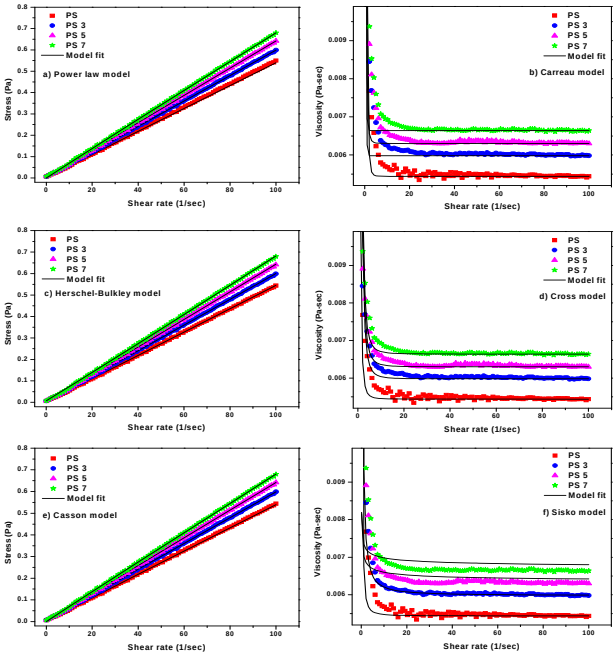

Fig. 4. (a-f) Rheological model fitting of PS blend solution at 20 °C

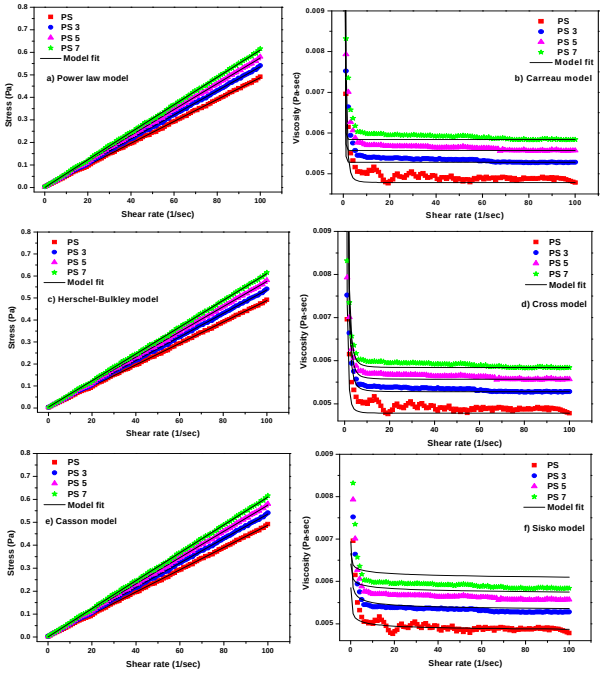

Fig. 5 (a-f) Rheological model fitting of PS blend solution at 30 °C

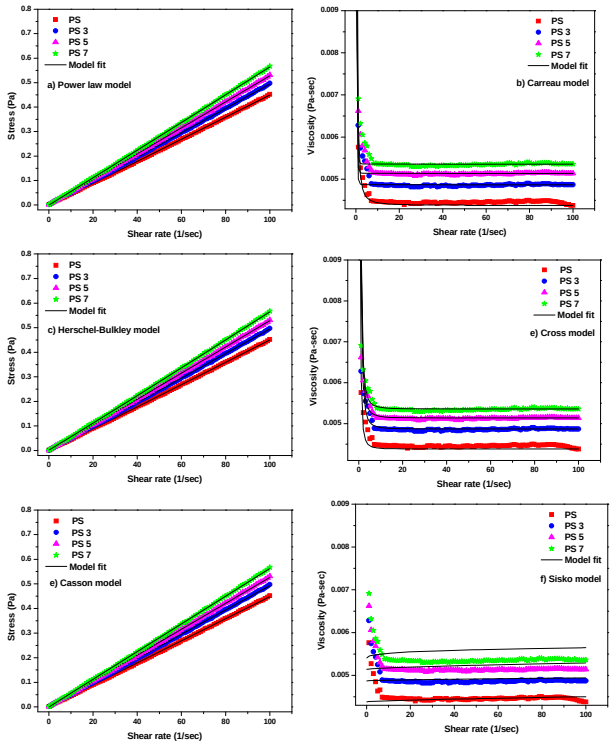

Fig. 6 (a-f) Rheological model fitting of PS blend solution at 40 °C

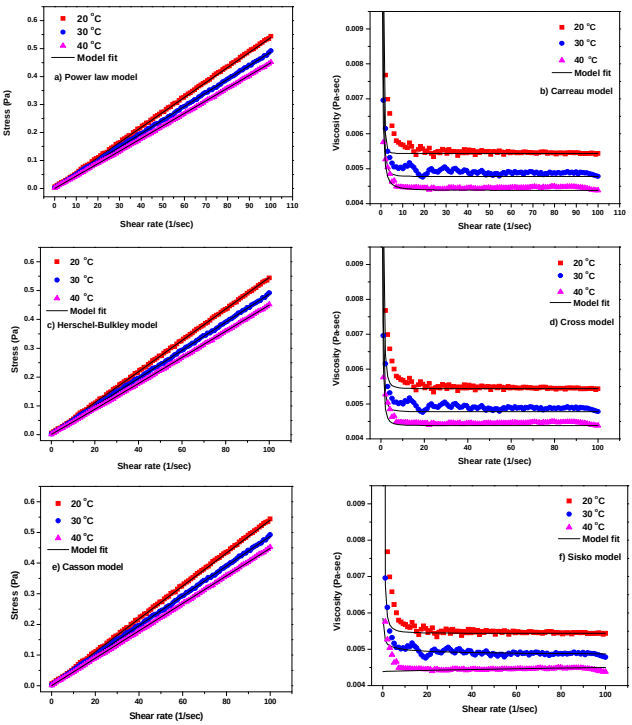

Fig. 7. (a-f) Rheological model fitting of PS solution at various temperatures

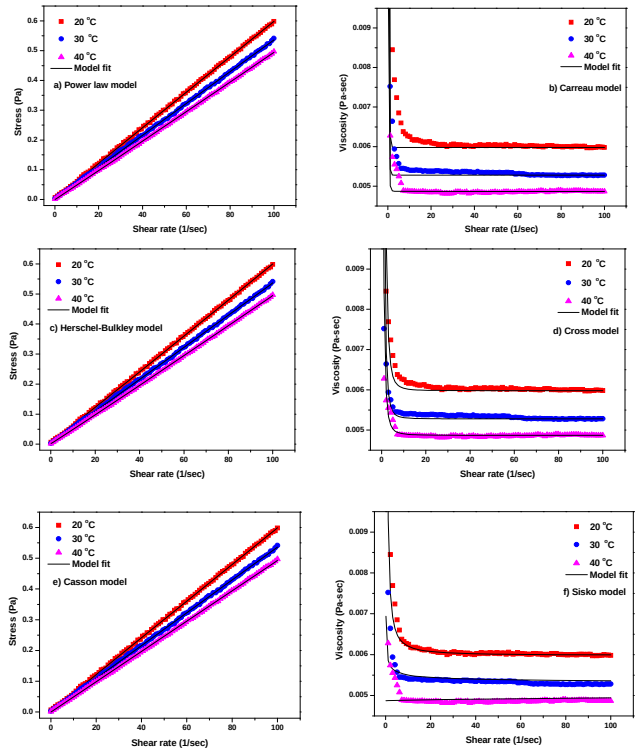

Fig. 8. (a-f) Rheological model fitting of PS 3 at various temperatures

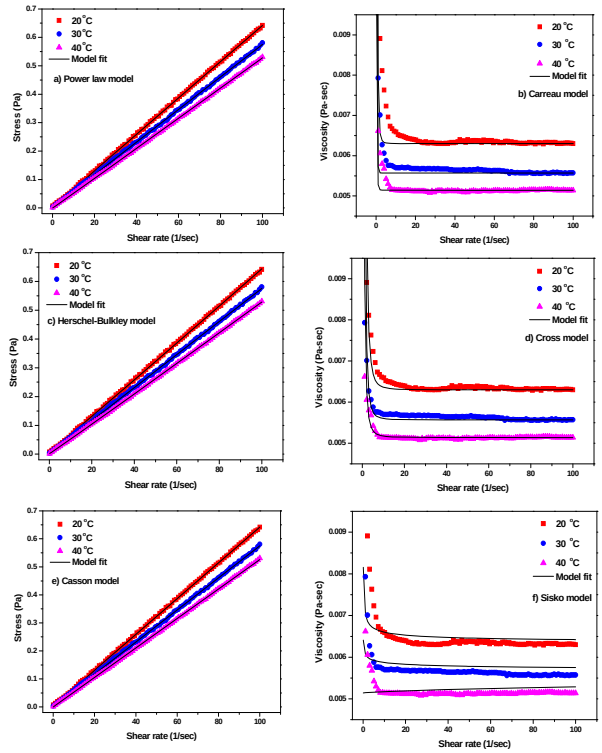

Fig. 9 (a-f) Rheological model fitting of PS 5 at various temperatures

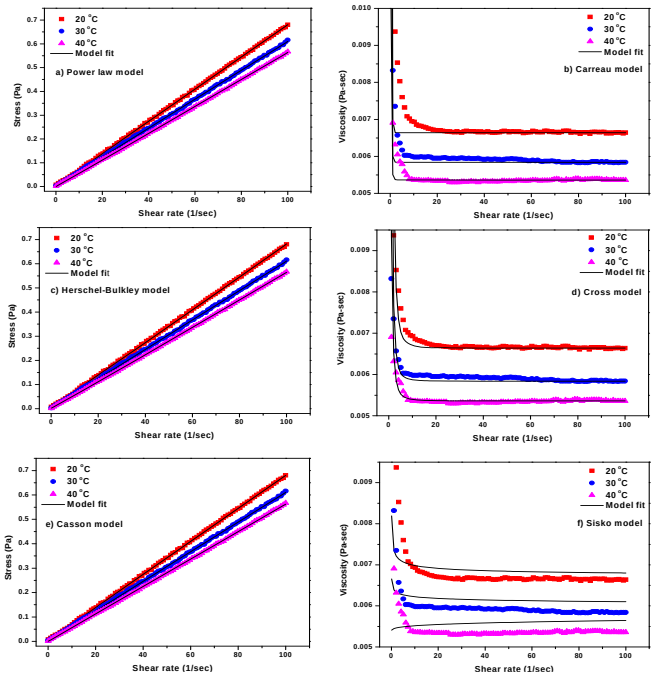

Fig. 10 (a-f) Rheological model fitting of PS 7 at various temperatures

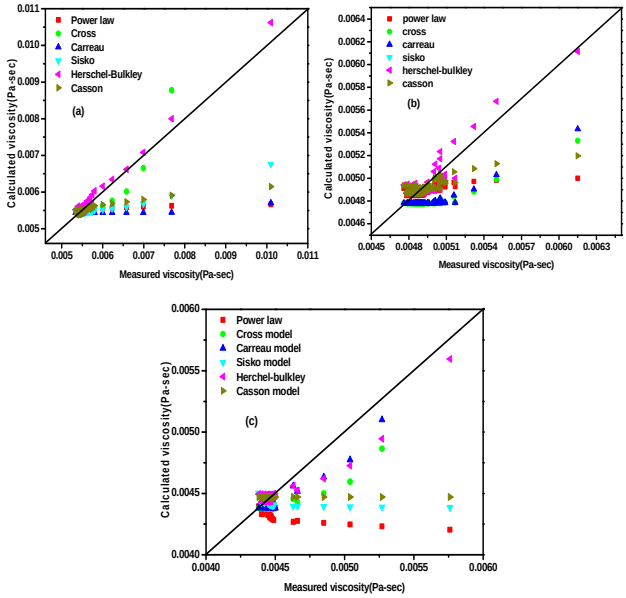

Fig. 11 (a-c) Measured Vs Calculated Viscosity comparison for pure PS solution at various temperatures, (a) 20 °C, (b) 30 °C and (c) 40 °C with different rheological models

6. Rheological models

Six models were proposed to study the viscosity of non-Newtonian fluids (Herschel-Bulkley Sisko, Power law, Carreau, Cross and Casson model) to fit the experimental data attained from the rheological behavior of pure PS and PS solutions with various concentration of Co-Al LDH at three different temperatures 20, 30 and 40 ^{o}C.

In this study, we have taken η_{∞}, η_{o} were known parameters at final and initial shear rate, respectively by considering them as viscosity. The obtained regression coefficient (R^2) values indicated that the Power law, Casson and Herschel-Buckley models are the best fit followed by Cross model. However, Sisko and Carreau model were not fitting with experimental data according to n value (see Table 2). Figs. 4-10 provide the appropriate information to know about the best fitted models. Models such as Power law and Casson model (R^2 nearby 1) are deviating from the line of equivalence (45° line). To validate this study, SE and B_f values are evaluated as given in Table 3. Figs. 11-14 shows the various rheological model with respect to pure PS and PS/Co-Al LDH blends, and justify weather the model is over predicted or under predicted. B_f >1 (over prediction); B_f <1 (under prediction) and B_f =1 were perfect model fitting with the experimental data. As displayed in Figs. 11-14, The pure PS solution closely followed the trend given by Herschel-Bulkley model at temperature of 20 ^{o}C and the Cross model best fits at temperature of 30 and 40 ^{o}C. On the other hand, Herschel-Buckley and Cross model described well the rheological data of PS solution with various concentration of Co-Al LDH obtained at lower (20 ^{o}C) and higher temperatures (30 and 40 ^{o}C), repectively. Bias factor (B_f) analysis demonstrates that the Power law and Casson model fit data are under predicting the measured value. Three models are suggested to relate the apparent viscosity to Co-Al LDH content, shear rate and temperature, which evidently affect the flow properties of the PS solution. The viscosity of the PS enhances exponentially with increasing Co-Al LDH content and falls exponentially with increasing temperature and shear rate.

Table 2. Linear regression parameters of PS/Co-Al LDH blend solutions for different rheological models.

Model	LDH loading (wt.%)	Temperature (^{o}C)	Parameters		R^2
			K	n	
Power law	0	20	0.0056	0.9891	0.9999
		30	0.0050	0.9928	0.9998
		40	0.0042	1.0098	0.9999
	3	20	0.0062	0.9905	0.9998
		30	0.0055	0.9928	0.9998
		40	0.0047	1.0098	0.9999
	5	20	0.0067	0.9905	0.9998
		30	0.0059	0.9928	0.9998
		40	0.0051	1.0098	0.9999
	7	20	0.0071	0.9905	0.9998
		30	0.0063	0.9928	0.9998
		40	0.0054	1.0098	0.9999
			C	m	
Cross	0	20	2.1061	2.7013	0.9979
		30	2.1222	2.5165	0.9941
		40	2.0623	2.1430	0.9901
	3	20	2.1065	2.6993	0.9980
		30	2.1123	2.6213	0.9972
		40	2.0689	2.2454	0.9938
	5	20	2.1061	2.6973	0.9980
		30	2.1140	2.6199	0.9971
		40	2.0620	2.2792	0.9948
	7	20	2.1059	2.7032	0.9981
		30	2.1130	2.6185	0.9971
		40	2.0646	2.2655	0.9944
			λ	n	
Carreau	0	20	1.2234	-3.5079	0.9963
		30	1.8874	-1.5653	0.9924
		40	2.7341	-0.5848	0.9906

Carreau	3	20	1.2324	-3.4630	0.9963
		30	1.5675	-2.2424	0.9955
		40	2.3546	-0.8725	0.9933
	5	20	2.0099	-0.6444	0.9738
		30	1.5716	-2.2338	0.9954
		40	2.2669	-0.9540	0.9941
	7	20	1.2175	-3.5386	0.9964
		30	1.5749	-2.2231	0.9954
		40	2.3085	-0.9150	0.9938
Sisko			**K**	**n**	
	0	20	1.57×10^{-3}	-0.6408	0.9999
		30	4.75×10^{-4}	0.6467	0.9998
		40	4.86×10^{-6}	1.6999	0.9999
	3	20	0.0037	-0.2239	0.9998
		30	0.0006	0.5623	0.9998
		40	3.72×10^{-6}	1.6436	0.9999
	5	20	0.0007	0.6046	0.9998
		30	0.0005	0.7778	0.9998
		40	7.57×10^{-6}	1.6477	0.9999
	7	20	0.0007	0.6725	0.9998
		30	0.0005	0.8356	0.9998
		40	8.56×10^{-5}	1.2606	0.9999
Herschel-Bulkley			**K**	**n**	
	0	20	5.0×10^{-3}	1.0163	0.9998
		30	4.70×10^{-3}	1.0064	0.9998
		40	4.12×10^{-3}	1.0181	0.9999
	3	20	0.0055	1.0162	0.9998
		30	0.0052	1.0064	0.9998
		40	0.0045	1.0181	0.9999
	5	20	0.0059	1.0162	0.9998
		30	0.0055	1.0064	0.9998
		40	0.0048	1.0181	0.9999
	7	20	0.0062	1.0162	0.9998
		30	0.0058	1.0064	0.9998
		40	0.0052	1.0181	0.9999
Casson			τ_o	η_∞	
	0	20	3.49×10^{-5}	5.30×10^{-3}	0.9999
		30	1.59×10^{-5}	4.82×10^{-3}	0.9998
		40	1.52×10^{-15}	4.47×10^{-3}	0.9998
	3	20	2.68×10^{-5}	0.0059	0.9998
		30	1.75×10^{-5}	0.0053	0.9998
		40	6.78×10^{-19}	0.0049	0.9998
	5	20	2.88×10^{-5}	0.0063	0.9998
		30	1.87×10^{-5}	0.0056	0.9998
		40	2.38×10^{-16}	0.0052	0.9998
	7	20	3.05×10^{-5}	0.0067	0.9998
		30	1.99×10^{-5}	0.0060	0.9998
		40	1.81×10^{-20}	0.0056	0.9998

Table 2. Bias Factor and Standard Error of different rheological models for predicting viscosity of PS/Co-Al LDH.

Model	Sample	Temperature (^oC)	Bias factor (B_f)	Standard error (SE)
Power law	PS	20	0.9540	0.0057
		30	0.9704	0.0024
		40	0.9570	0.0012
	PS 3	20	0.9603	0.0062
		30	0.9872	0.0026
		40	0.9861	0.0013
	PS 5	20	0.9793	0.0066
		30	1.0027	0.0027
		40	0.9985	0.0014

Power law	PS 7	20	0.9866	0.0069
		30	1.0145	0.0029
		40	1.0224	0.0014
Cross	PS	20	0.9984	0.0012
		30	0.9720	0.0002
		40	0.9820	0.0001
	PS 3	20	0.9967	0.0011
		30	0.9964	0.0004
		40	1.0043	0.0002
	PS 5	20	0.9982	0.0012
		30	0.9952	0.0005
		40	1.0045	0.0002
	PS 7	20	1.0004	0.0013
		30	0.9951	0.0005
		40	1.0043	0.0003
Carreau	PS	20	0.9690	0.0031
		30	0.9730	0.0002
		40	0.9850	0.0001
	PS 3	20	0.9679	0.0034
		30	0.9769	0.0014
		40	0.9893	0.0007
	PS 5	20	0.9719	0.0035
		30	0.9758	0.0015
		40	0.9897	0.0007
	PS 7	20	0.9716	0.0037
		30	0.9756	0.0016
		40	0.9894	0.0008
Sisko	PS	20	0.9824	0.0013
		30	0.9782	0.0024
		40	0.9790	0.0012
	PS 3	20	0.9927	0.0002
		30	0.9922	0.0025
		40	0.9901	0.0013
	PS 5	20	0.9830	0.0064
		30	1.0045	0.0027
		40	0.9989	0.0014
	PS 7	20	0.9893	0.0068
		30	1.0158	0.0028
		40	1.0225	0.0014
Herschel-Bulkley	Pure PS	20	1.0030	0.0005
		30	1.0023	0.0005
		40	1.0090	0.0004
	PS 3	20	1.0035	0.0005
		30	1.0173	0.0006
		40	1.0091	0.0007
	PS 5	20	1.0233	0.0007
		30	1.0333	0.0007
		40	1.0219	0.0008
	PS 7	20	1.0309	0.0008
		30	1.0454	0.0008
		40	1.0463	0.0008
Casson	Pure PS	20	0.9590	0.0054
		30	0.9784	0.0023
		40	0.9830	0.0012
	PS 3	20	0.9658	0.0060
		30	0.9926	0.0024
		40	0.9913	0.0013
	PS 5	20	0.9848	0.0063
		30	1.0081	0.0026
		40	1.0050	0.0014
	PS 7	20	0.9922	0.0066
		30	1.0201	0.0027
		40	1.0291	0.0014

Figs. 11-14 justify that the correlations given in this work fit better with experimental values than that of Rosenberger et al. [43] in the whole range of parameters (Co-Al (0-0.35 g), temperature (20, 30 and 40 °C) and shear rate (0.1-100 s^{-1}). This property is used especially in the course of transporting, mixing, handling and processing. These models are especially useful in hydrodynamic optimization and also computational fluid dynamic (CFD) simulation of airlift where viscosity plays a major role on the hydrodynamic regime, oxygen transfer and mass transport and consequently, influences the system performance [44].

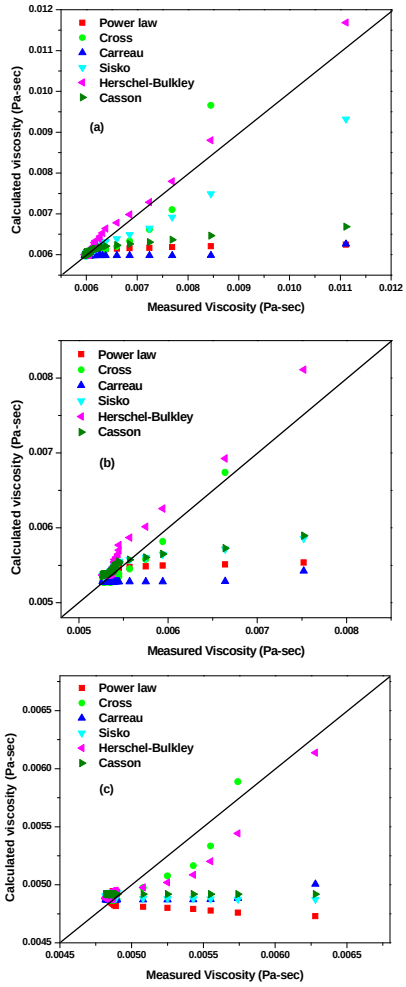

Fig. 12. (a-c) Measured Vs Calculated Viscosity comparison for PS 3 solution at various temperatures, (a) 20 °C, (b) 30 °C and (c) 40 °C with different rheological

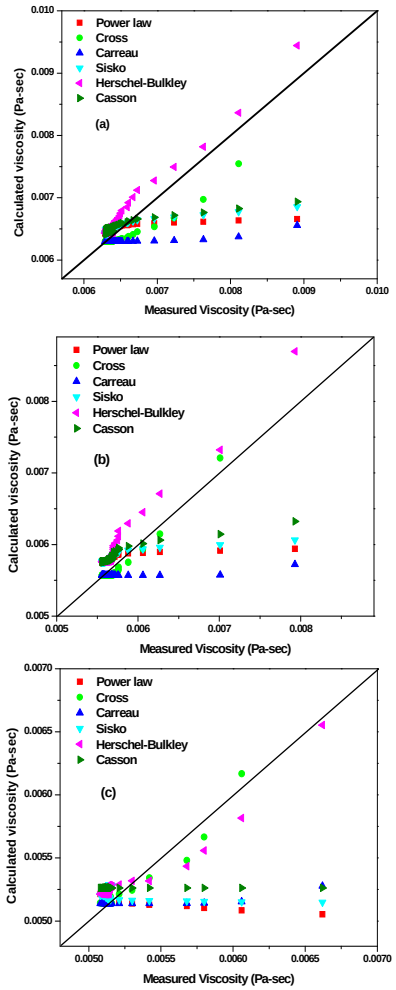

Fig. 13. (a-c) Measured Vs Calculated Viscosity comparison for PS 5 solution at various temperatures, (a) 20 °C, (b) 30 °C and (c) 40 °C with different rheological

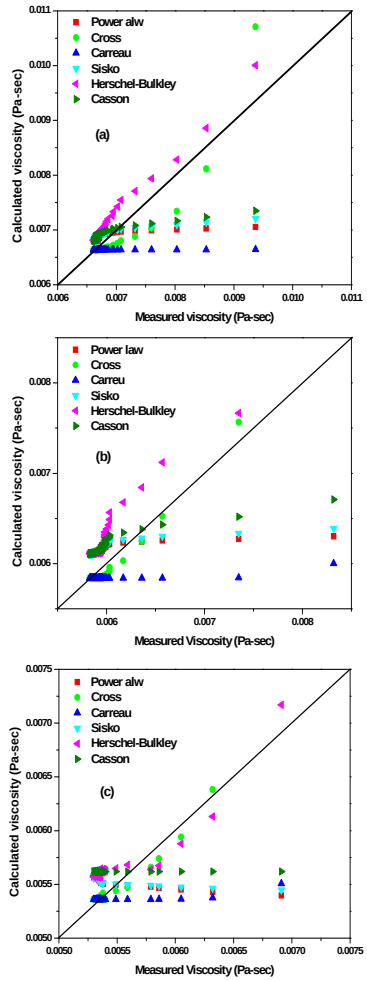

Fig. 14. (a-c) Measured vs. Calculated Viscosity comparison for PS 7 solution at various temperatures, (a) 20 °C, (b) 30 °C and (c) 40 °C with different rheological

7. Conclusions

Using co-precipitation technique, organically modified Co-Al LDH was successfully prepared. The effect of LDH loading with temperature on the rheological behavior of PS/Co-Al LDH blends has been effectively studied, which is crucial for polymer manufacturing industries. The XRD analysis affirmed the d-spacing value of modified Co-Al LDH layers. FTIR analysis proved the existence of sulfate group in the organically modified Co-Al LDH. Rheological studies displayed the increment in viscosity by increasing the LDH loading in the polymer solution. The viscosity of PS and PS/Co-Al LDH solution rapidly decreased with increasing the shear rate for all the applied temperatures. Rheology data of PS and PS/Co-Al LDH solution were validated with different rheological models such as Herschel-Bulkley, Power law, Sisko, Casson, Carreau and Cross model to assess the flow behavior of PS solution. Based on regression coefficient and B_f values, it can be concluded that for both pure Ps and various PS/LDH blend solution, Herschel-Buckley model displays good fit with reological data obtained at lower temperature (20 °C), whereas Cross model offers best fit at higher temperatures (30 and 40 °C).

References

[1] A. Usuki, Y. Kojima, M. Kawasumi, A. Okada, A. Fujushima, T. Kurauchi, O. Kamigaito, J. Mater. Res. 8 (1993) 1179-1184.
[2] A. Loganathan, K. Kumar, Appl. Nanosci. 6 (2016) 629-639.
[3] Y. Kojima, A. Fujushima, A. Usuki, A. Okada, T. Kurauchi, J. Mater. Sci. Lett. 12 (1993) 889-890.
[4] S. S. Ray, M. Okamoto, Prog. Polym. Sci. 28 (2003) 1539-1641.
[5] B.M. Choudary, M.L. Kantam, V. Neeraja, K.K. Rao, F. Figueras, L. Delotte, Green Chem. 3 (2001) 257-260.
[6] B.M. Choudary, S. Madhi, N.S. Chowdari, M.L. Kantam, B. Sreedhar, J. Amer. Chem. Soc. 124 (2002) 14127-14136.
[7] Y. You, H. Zhao, G.F. Vance, Appl. Clay Sci. 21 (2002) 217-226.
[8] N. Kozai, T. Ohnuki, S. Komarneni, J. Mater. Res. 17 (2002) 2993-2996.
[9] J.H. Choy, S.Y. Kwak, Y.J. Jeong, J.S. Park, Chem Int Ed 39 (2000) 4042-4045.
[10] J. Qiu, G. Villemure, J. Electroanal. Chem. 428 (1997) 165-172.
[11] H.F.W. Taylor, Mineral Mag. 39 (1973) 377-389.
[12] T. Kameda, K. Hoshi, T. Yoshioka, Solid State Sci. 17 (2013) 28-34.
[13] Qi. Tao, Y. Zhang, X. Zhang, Y. Peng, H. He, J. Solid State Chem. 179 (2006) 708-715.
[14] L. Qiu, W. Chen, B. Qu, Polym. Degrad. Stab. 87 (2005) 433-440.
[15] L. Qiu, B. Qu, J. Colloid Interface Sci. 301 (2006) 347-351.
[16] P. Ding, B. Qu, J. Colloid Interface Sci. 291 (2005) 13-18.
[17] F.A. He, L.M. Zhang, F. Yang, L.S. Chen, Q. Wu, J. Polym Res. 13 (2006) 483-493.
[18] G.A. Wang, C.C. Wang, C.Y. Chen, Polym. Degrad. Stab. 91 (2006) 2443-2450.
[19] L. Du, B. Qu, M. Zhang, Polym. Degrad. Stab. 92 (2007) 497-502.
[20] M. Zhang, P. Ding, L. Du, B. Qu. Mater. Chem. Phys. 109 (2008) 206-211.
[21] S.M. Al-Zahrani, T.F. Al-Fariss, Chem. Eng. Process. 37 (1998) 433-437.
[22] M.A. Rao, Viscoelastic Properties of Foods. Elsevier Applied Science, London, 1992.
[23] M.B. Zakaria, Z.A. Rahman, Carbohydr. Polym. 29 (1996) 25-27.
[24] R.K. Wanchoo, S.K. Sharma, R. Bansal, J. Polym. Mate. 13 (1996) 49-55.
[25] M.J. Solomon, A.S. Almusallam, K.F. Seefeldt, A. Somwangthanaroj, P. Varadan, Macromolecules. 34 (2001) 1864-1872.
[26] C.A. Mitchell, R. Krishnamoorti, J. Polym. Sci., Part B: Polym. Phys. 40 (2002) 1434-1443.
[27] Y. Ohta, H. Sugiyama, H. Yasuda, J. Polym. Sci., Part B: Polym. Phys. 32 (1994) 261-269.
[28] B. Briscoe, P. Luckham, S. Zhu, Polymer. 41 (2000) 3851-3860.
[29] R. Perez, E. Rojo, M. Fernandez, V. Leal, P. Lafuente, A. Santamaria, Polymer. 46 (2005) 8045-8053.
[30] T.F. Al-Fariss, I. J. Eng Sci. 14 (1988) 231-245.
[31] PP. Kundu, M. Kundu, Polymer. 42 (2001) 2015-2020.
[32] F.R. Costa, U. Wagenknecht, D. Jehnichen, M.A. Goad, G. Heinrich, Polymer. 47 (2006)1649-1660.
[33] A.W. Sisko, Ind Eng Chem. 50 (1958) 1789-1792.
[34] N. Casson, Rheology of disperse systems, Pergamon press, London, 1959 pp 84-102.
[35] M.M. Cross, J. Colloid Sci. 20 (1965) 417-437.
[36] P.J. Carreau, I.F. MacDonald, R.B. Bird, Chem. Eng. Sci. 23 (1968) 901-911.
[37] C.I. Nindo, J. Tang, J.R. Powers, P.S. Takhar, LWT Food Sci Tech. 40 (2007) 292-299.
[38] G.D. Betts, S.J. Walker, Verification and validation of food spoilage models. in: R. Steele (Ed.), Understanding and measuring shelf life of food, CRC Press, 2004 pp. 184-217.
[39] F.R. Costa, A. Leuteritz, U. Wagenknecht, D. Jehnichen, L. Haubler, G. Heinrich, Appl. Clay Sci. 38 (2008) 153-164.
[40] S. Guo, C. Zhang, H. Peng, W. Wang, T. Liu, Compos. Sci. Technol. 71 (2011) 791-796.
[41] S. Kanan, C.S. Swamy, J. Mater. Sci. Lett. 11 (1992) 1585-1587.
[42] S. Mallakpour, M. Dinari, J. Therm. Anal. Calorim. 119 (2015)1123-1130.
[43] S. Rosenberger, K. Kubin, M. Kraume, Eng Life Sci. 2 (2002) 269-275.
[44] A.K. Garakani, M.R. Mehrnia, N. Mostofi, M.H. Sarrafzadeh, Process Biochem 46 (2011) 1138-1145.